Hydrogen Peroxide Formation during Iron Deposition in Horse Spleen Ferritin Using O_2 as an Oxidant†

Stuart Lindsay, David Brosnahan, and Gerald D. Watt*

Department of Chemistry and Biochemistry, Brigham Young University, Provo, Utah 84602

Received August 21, 2000; Revised Manuscript Received January 23, 2001

ABSTRACT: The reaction of Fe^{2+} with O_2 in the presence of horse spleen ferritin (HoSF) results in deposition of $Fe(OH)_3$ into the hollow interior of HoSF. This reaction was examined at low Fe^{2+}/HoSF ratios (5−100) under saturating air at pH 6.5−8.0 to determine if H_2O_2 is a product of the iron deposition reaction. Three methods specific for H_2O_2 detection were used to assess H_2O_2 formation: (1) a fluorometric method with emission at 590 nm, (2) an optical absorbance method based on the reaction $H_2O_2 + 3I^- + 2H^+ = I_3^- + 2H_2O$ monitored at 340 nm for I_3^- formation, and (3) a differential pulsed electrochemical method that measures O_2 and H_2O_2 concentrations simultaneously. Detection limits of 0.25, 2.5, and 5.0 μM H_2O_2 were determined for the three methods, respectively. Under constant air-saturation conditions (20% O_2) and for a 5−100 Fe^{2+}/HoSF ratio, Fe^{2+} was oxidized and the resulting Fe^{3+} was deposited within HoSF but no H_2O_2 was detected as predicted by the reaction $2Fe^{2+} + O_2 + 6H_2O = 2Fe(OH)_3 + H_2O_2 + 4H^+$. Two other sets of conditions were also examined: one with excess but nonsaturating O_2 and another with limiting O_2. No H_2O_2 was detected in either case. The absence of H_2O_2 formation under these same conditions was confirmed by microcoulometric measurements. Taken together, the results show that under low iron loading conditions (5−100 Fe^{2+}/HoSF ratio), H_2O_2 is not produced during iron deposition into HoSF using O_2 as an oxidant. This conclusion is *inconsistent* with previous, carefully conducted stoichiometric and kinetic measurements [Xu, B., and Chasteen, N. D. (1991) *J. Biol. Chem. 266*, 19965], predicting that H_2O_2 is a quantitative product of the iron deposition reaction with O_2 as an oxidant, even though it was not directly detected. Possible explanations for these conflicting results are considered.

Ferritins are 24-subunit proteins distributed throughout nature that are responsible for oxidizing, depositing, and storing free and potentially harmful Fe^{2+} in their hollow interiors as an iron(III) mineral core of ferrihydrite (*1*−*5*). The 24-mers are assembled from antiparallel dimer subunit pairs that form an approximate rhombic dodecahedral structure with a hollow interior 80 Å in diameter surrounded by a protein shell 20 Å thick (*2*, *6*). Eight hydrophilic channels located at the intersection of three subunits connect the exterior solution with the ferritin interior and are thought to be pathways through which iron enters and leaves the ferritin interior during the iron deposition and release reactions. Both iron deposition and release are redox reactions involving the one-electron interconversion of Fe^{2+} and Fe^{3+} and require external oxidants and reductants to interact with the protein to conduct the ferritin-associated redox reactions (*3*, *7*). Although essential to the functioning of ferritin, the redox reactions associated with iron deposition and release remain poorly understood, particularly, with regard to how the redox reagents interact with Fe^{2+} bound to the protein or with $Fe(OH)_3$ contained as a mineral core within the ferritin interior and transfer electrons during the catalytic process. Progress toward better understanding the iron deposition reaction was made by the observation and subsequent study of a μ-dioxodiiron site (ferroxidase center) found within the ferritin H subunit that is proposed to catalyze Fe^{2+} oxidation by O_2 (*8*, *9*). However, details of how the ferroxidase center functions during the ferritin-catalyzed iron deposition reaction have remained obscure.

Recent studies using pH-stat methods, mass spectrometry, O_2-electrode oximetry, and Mössbauer spectroscopy have investigated (*10*−*14*) the iron deposition reaction in detail using O_2 as an oxidant and suggest that early Fe^{2+} oxidation by HoSF[1] at low iron loading levels (~10 Fe^{2+}/HoSF ratio) is described by reaction 1. At higher iron loading levels when larger iron cores are present, the Fe^{2+}/O_2 stoichiometry steadily increases from 2.0 to a limiting maximum value of 4.0 (*14*) as described by reaction 2.

$$2Fe^{2+} + O_2 + 6H_2O = 2Fe(OH)_3 + H_2O_2 + 4H^+ \quad (1)$$

$$4Fe^{2+} + O_2 + 10H_2O = 4Fe(OH)_3 + 8H^+ \quad (2)$$

At low Fe^{2+}/HoSF ratios, the ferroxidase center in the H subunit of animal ferritin is proposed to initially function

† This research was supported by Research Grant 5RO1 DK36799-05 from the National Institutes of Health awarded to G.D.W. Additional support was received from the College of Mathematics and Physical Science at Brigham Young University to support undergraduate research.

* To whom correspondence should be addressed. Phone: (801) 378-4561. Fax: (801) 378-5474. E-mail: gdwatt@chemdept.byu.edu.

[1] Abbreviations: HoSF, horse spleen ferritin; DPP, differential pulsed polarography; BSA, bovine serum albumin; Mops, 3-(*N*-morpholino)-propanesulfonic acid; EDTA, ethylenediaminetetraacetic acid; PO_2, O_2 partial pressure.

10.1021/bi001981v CCC: $20.00
Published on Web 02/23/2001

during iron oxidation, and as shown by reaction 1, H_2O_2 is expected to be the dominant product of O_2 reduction (*10*, *14*). At higher Fe^{2+}/HoSF ratios, when sufficient iron mineral core is present to presumably catalyze Fe^{2+} oxidation, the mechanism and consequently the stoichiometry for HoSF iron deposition change to reaction 2 and H_2O is the predominant product of O_2 reduction. Intermediate iron loading levels were shown to give Fe^{2+}/O_2 ratios between 2.0 and 4.0, suggesting reactions 1 and 2 are occurring simultaneously and contribute to the overall stoichiometry. Consistent with this view are experiments conducted in the presence of catalase showing that only reaction 2 occurs, presumably due to catalase decomposing H_2O_2 into O_2, which is recycled through the catalytic process (*10*, *14*, *15*).

The view that two mechanistically distinct Fe^{2+} oxidation reactions (eqs 1 and 2) occur during iron deposition is relevant for understanding iron deposition in ferritins using O_2 as an oxidant. As part of a program to investigate iron deposition in HoSF, we conducted kinetic measurements to evaluate the proposed reactivity of the ferroxidase center and the mineral core surface to determine the rate constants and the contributions of each to the overall iron deposition reaction. To conduct and interpret these kinetic measurements, it was necessary to understand the catalytic events occurring during the formation of H_2O_2, proposed (*10*, *14*) to occur at the ferroxidase center, and compare them to the catalytic reduction of O_2 to H_2O, proposed to occur on the mineral core surface. Here we report extensive measurements attempting to verify and quantitate the production of H_2O_2 formed at the ferroxidase center (reaction 1) during iron deposition in HoSF at low iron loading levels. Despite extensive studies predicting the formation of H_2O_2 at low iron loading levels using O_2 as an oxidant (*10*, *11*, *13*, *14*), the results reported here do not confirm the formation of H_2O_2 under any of the conditions examined during iron deposition in HoSF.

MATERIALS AND METHODS

Apo horse spleen ferritin (HoSF) was purchased from Sigma, and reduction with dithionite and chelation with bipyridine (bipy) removed residual iron to yield a ratio of 0.3−1.0 Fe/HoSF. Stock apo HoSF solutions (35−50 mg/mL) were prepared in 0.025 M Mops and 0.050 M NaCl (pH 7.5) and diluted to appropriate concentrations as described below. Protein concentrations were determined by the Lowry method after calibration with standard bovine serum albumin (BSA). Fe^{2+} was present as $[Fe(bipy)_3]^{2+}$ (ϵ_{520} = 8400 M^{-1} cm^{-1}). Vacuum Atmospheres gloveboxes containing N_2 (<0.10 ppm O_2) were used to prepare air-sensitive solutions or to conduct reactions requiring anaerobic conditions. Aqueous 12.5 mM Fe^{2+} stock solutions at pH 3.0 were prepared from ferrous sulfate and stored in a Vacuum Atmospheres glovebox.

H_2O_2 Assessments. Iron deposition reactions were conducted under three sets of conditions at 25 °C with varying amounts of O_2 supplied by air as the oxidant. In all three types of experiments, HoSF was typically 5.7 μM in 0.025 M Mops containing 50 mM NaCl at pH values between 6.5 and 8.0. For the first, the reaction mixture was rapidly stirred in air and then 5, 10, 50, or 100 Fe^{2+}/HoSF were added using an anaerobic 12.5 mM Fe^{2+} solution. For the other two experiments, O_2 was in moderate excess (4.0 Fe^{2+}/O_2) or in stoichiometric amounts (2.0 Fe^{2+}/O_2). For these latter experiments, the same reaction mixture was first made anaerobic in sealed 5.0 mL vials under N_2 and rapidly stirred and then the appropriate amounts of gaseous air or an aqueous solution saturated with air was added. The saturated air solution was standardized prior to use using microcoulometry at −560 mV at which potential O_2 is reduced to H_2O. For use of gaseous additions of air, it was assumed that air contained 24.58 mL/mmol at 298 K and was 20% O_2. The reactions were carried out for 10−30 min, a time interval that was sufficient for oxidation of all Fe^{2+} to Fe^{3+}. During this reaction interval, 50 μL samples of the reaction mixture were removed for H_2O_2 assessment. Three independent methods were then used to determine the amount of H_2O_2 formed during iron deposition reactions catalyzed by HoSF.

Fluorometry (Method 1). Hydrogen peroxide was quantified by using an Amplex Red Hydrogen Peroxide Assay Kit including a standard 3.5% H_2O_2 solution from Molecular Probes (Eugene, OR). The reaction is based on detecting H_2O_2 using 10-acetyl-3,7-dihydroxyphenoxazine (Amplex Red reagent), a highly sensitive and stable probe for H_2O_2. In the presence of horseradish peroxidase, the Amplex Red reagent reacts with H_2O_2 with a 1/1 stoichiometry to produce fluorescent resorufin with emission at 590 nm (*16*).

Initial Fe^{2+} oxidation by HoSF was conducted at pH 7.5 as a function of time to determine when H_2O_2 was produced. At an iron to HoSF ratio of 5.0, 50 μL samples were removed at 10 s intervals. For larger iron to HoSF ratios, where more time was necessary to reach completion, samples were removed after 30 s and at ∼100 s intervals. These samples were immediately frozen in liquid nitrogen in 500 μL microcentrifuge tubes and stored at −80 °C for later analysis. Immediately after each 50 μL sample was thawed, 100 μL of 400 μM Amplex Red reagent was added, and 30 min later, emission spectra were recorded using a Perkin-Elmer LS50B luminescence spectrometer with excitation at 560 nm. In reactions or experimental controls where high levels of Fe^{2+} were present, excess emission was observed. Addition of 25 μL of 2 mM EDTA removed this interference. To maintain consistency, EDTA was added immediately before freezing to all controls, samples, and standards.

I_3^- Formation Using Acidified KI (Method 2). Hydrogen peroxide was quantified using an optical absorbance method based on the reaction $H_2O_2 + 3I^- + 2H^+ = I_3^- + 2H_2O$. A solution of 0.01 M potassium iodide in 1.0 M HCl was reacted with H_2O_2 to produce I_3^-, which absorbs at 340 nm (ϵ = 2600 M^{-1} cm^{-1}). Due to moderate oxygen sensitivity, the acidified KI solution was kept in a glovebox under a nitrogen atmosphere. To prevent optical interference from holo HoSF at high iron loading levels, the solution was separated from HoSF by spinning at 1000 rpm in Centricon centrifuge concentrators (Amicon, Beverly, MA) with a 100 kDa membrane. The protein-free solution (200 μL) was made anaerobic, to which 800 μL of acidified KI was added. The samples were read at 340 nm in the glovebox with a Milton Roy Spectronic 401 spectrometer. In some cases, this reaction was also performed aerobically with freshly prepared reagents being added to reaction samples after iron deposition into HoSF. Precipitated HoSF was removed by centrifugation, and samples were read at 340 nm using the HP 8453 diode array spectrometer.

Differential Pulsed Polarography (DPP, Method 3). H_2O_2, O_2, and Fe^{2+} concentrations were measured using a Princeton Applied Research model 303 SMDE in the differential pulsed mode attached to a chart recorder. Oxygen, H_2O_2, and Fe^{2+} are all rapidly reduced at a dropping mercury electrode at peak potentials at pH 7.5 of −170, −1065, and −1350 mV relative to a saturated calomel electrode, respectively. Buffer was first added to the reaction vessel and made anaerobic by bubbling with argon. A scan at 5.0 mV/s was taken in the DPP mode from 0.0 to −1.5 V to establish a baseline. Next, 5.7 μM apo HoSF and varying amounts of air-saturated buffer were added, and another scan was taken. Finally, Fe^{2+} was added and allowed to react for 10 min before a final scan was taken. From current measurements at the indicated potentials, O_2, H_2O_2, and Fe^{2+} concentrations were determined.

Microcoulometry. Microcoulometry was conducted using previously described methods (*17*, *18*). A reduction potential of −560 mV was used to quantitatively reduce Fe^{3+}, O_2, and H_2O_2 to Fe^{2+} and H_2O, respectively. A total reduction sensitivity of 0.10 μM was determined. Excess O_2 was removed from all samples prior to microcoulometric measurements by several evacuation-flush cycles using purified N_2.

Fe^{3+} Deposition in HoSF Using H_2O_2 as an Oxidant. Iron deposition reactions were conducted as described above for O_2 as the oxidant except all samples were first made anaerobic, and appropriate amounts of standardized H_2O_2 were added to oxidize Fe^{2+}/HoSF ratios of 10, 50, or 100 followed immediately by addition of a standardized Fe^{2+} solution. Control reactions were conducted in an identical manner except HoSF was absent.

RESULTS

Three direct and specific methods for H_2O_2 assessment were used to determine the amount of H_2O_2 formed during the iron deposition reaction catalyzed by HoSF using O_2 as an oxidant under various conditions.

Fluorometric Assessment of H_2O_2 Using Amplex Red (Method 1). A standard curve from 0 to 10 μM H_2O_2 for the addition of H_2O_2 to 1.0 μM HoSF in 0.025 M Mops and 0.05 M NaCl (pH 7.5) was determined from which a value of 0.25 μM was calculated for the H_2O_2 detection limit.[2] The fluorescence emission maximum (λ_{max}) occurs at 590 nm, a position far removed from possible sources of protein or iron core interference. The small characteristic background emission spectrum, which is observed when fluorometric reagents, HoSF, and buffer are mixed in air in the absence of added H_2O_2, was subtracted from every H_2O_2 control and sample reaction. Similar reactivity and detection limits were determined at pH 6.5, making it possible to conduct reliable H_2O_2 assessments for HoSF-catalyzed reactions as a function of pH. Similar standard addition measurements with the same detection limit were also conducted in the presence of holo HoSF containing a small mineral core with a Fe^{3+}/HoSF ratio of 5−100 that demonstrated that H_2O_2 is readily assessed in the presence of holo HoSF.

H_2O_2 Assessments Using Acidified KI (Method 2). A standard curve for the addition of 0−50 μM H_2O_2 to acidified I^- to produce I_3^-in the presence of apo HoSF was linear, producing a detection limit of 2.5 μM for H_2O_2. Because the absorbance of I_3^- is measured at 340 nm, there is little interference from apo HoSF. However, when large amounts of iron are deposited, the absorbance of the core at 340 nm limits the utility of this method. For the small core sizes (5−100 Fe^{3+}/HoSF) investigated below, little interference was encountered. This method is also independent of the pH at which the iron deposition reaction is conducted and is reliable for HoSF assessments conducted as a function of pH. Because this method requires 1.0 M HCl for development of I_3^-, it offers the advantage of acid quenching any peroxo intermediates that might be bound to HoSF and releasing them as H_2O_2.

H_2O_2 Assessment using Differential Pulsed Polarography (DPP, Method 3). O_2 and H_2O_2 are rapidly reduced at a dropping mercury electrode at peak potentials of −170 and −1095 mV, respectively. A standard curve was obtained under anaerobic conditions for the addition of H_2O_2 to apo HoSF at pH 7.5, giving a detection limit of 5.0 μM. Anaerobic conditions are required because in the presence of O_2, H_2O_2 is formed at the electrode in proportion to the amount of O_2 present and interferes with H_2O_2 assessments. Linearity is observed for H_2O_2 concentrations up to 100 μM, making this method both sensitive and useful for H_2O_2 assessments over wide concentration ranges. Using DPP at −170 mV, a standard curve for O_2 was obtained with a detection limit of 14 μM. At −1350 mV under the same anaerobic conditions, Fe^{2+} is reduced to Fe at the mercury electrode and its concentration is readily determined, making it possible, under appropriate conditions, to simultaneously assess O_2, H_2O_2, and Fe^{2+} as either reactants or products formed during HoSF-catalyzed reactions.

H_2O_2 Production under Air-Saturation Conditions. Figure 1 compares the expected and observed production of H_2O_2 during HoSF-catalyzed iron deposition conducted under saturating air by the three methods discussed above. Identical reaction conditions were chosen to produce 28 μM H_2O_2 according to reaction 1 when 10 Fe^{2+}/HoSF was oxidized. Figure 1 shows that the amount of H_2O_2 actually measured during the iron deposition reaction is the same as controls conducted in the absence of H_2O_2. These results indicate that H_2O_2 is not a product of the HoSF iron deposition reaction with saturating air as an oxidant. These three methods are based on different detection principles for H_2O_2 assessment and are not subject to the same types of interference, so the results confidently demonstrate the absence of H_2O_2 production under the conditions that were examined. The results shown in Figure 1 are for the addition of 10 Fe^{2+} to HoSF and correspond to 2.2 Fe^{2+}/heavy subunits present in the HoSF sample (4 H subunits/HoSF). Using the more sensitive fluorometric method, no H_2O_2 was observed when 5.0 Fe^{2+}/HoSF were oxidized (1.1 Fe^{2+}/heavy subunit). These conditions should give near-maximal production of H_2O_2, according to reaction 1, if it is produced at the ferroxidase center present in the heavy subunit (*10*, *14*).

The results depicted in Figure 1 were obtained after a 10 min reaction interval, and the possibility that H_2O_2 was formed earlier in the reaction but decomposed before being assessed at 10 min was examined. Hydrogen peroxide assessments at an Fe^{2+}/HoSF ratio of 5.0 were conducted from as early as 10−600 s with samples removed every 30−

[2] The detection limit (DL) is given by the relation $DL = 3\sigma/(N)^{1/2}$, where σ is the standard deviation and N is the number of measurements.

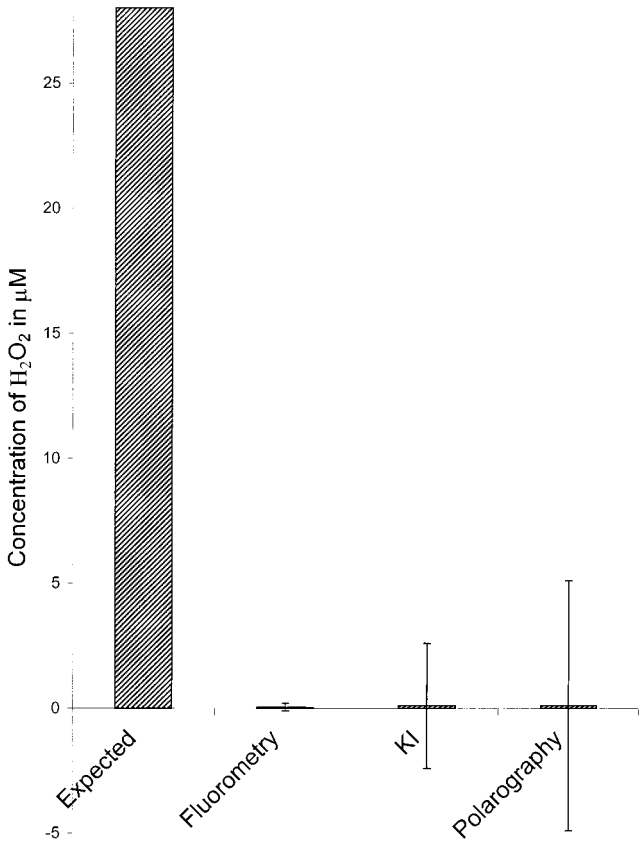

FIGURE 1: Determination of the amount of H_2O_2 for a reaction conducted with 5.7 μM HoSF in 0.025 M Mops (pH 7.5) as determined by methods 1−3 under conditions that would form 28 μM H_2O_2 according to reaction 1.

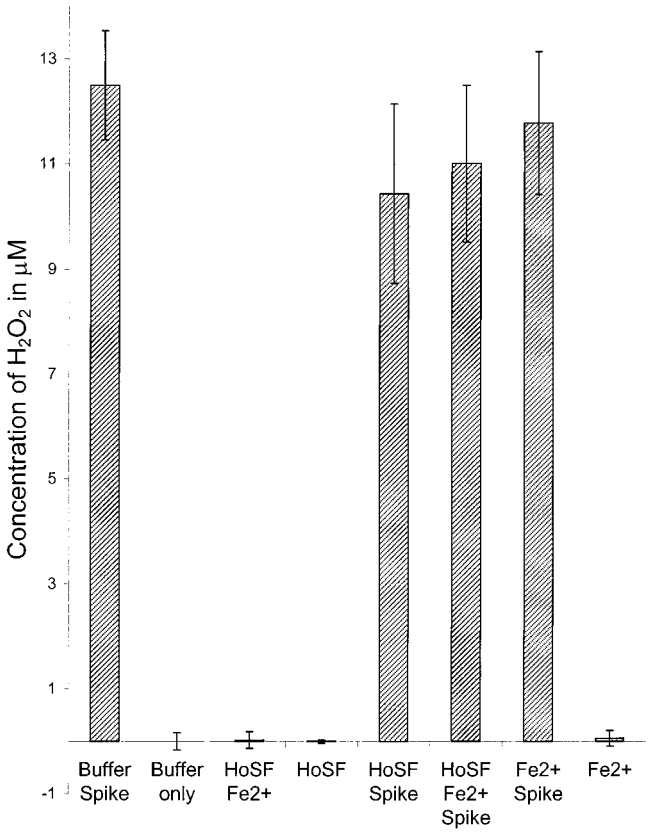

FIGURE 2: Assessment of H_2O_2 formation shown in lane 3 using method 1 with a limiting Fe^{2+}/O_2 ratio of 2.0 and an Fe^{2+}/HoSF ratio of 10.0. A standard addition of H_2O_2 to a concentration of ~12 μM was made to lanes 1 and 5−7. Control reactions with no added H_2O_2 are shown in lanes 2, 4, and 8. The reactions were conducted at pH 7.5 with 5.7 μM HoSF.

100 s, but no H_2O_2 was detected. Other Fe^{2+}/HoSF ratios were likewise examined, but with methods 1 and 2, no H_2O_2 was detected from 30 to 600 s.

Additional experiments were conducted to evaluate the effect of making larger additions of Fe^{2+} to HoSF under air-saturating conditions. When 50 or 100 Fe^{2+} were added under the conditions described in the legend of Figure 1, the results showed that addition of larger quantities of Fe^{2+} did not enhance H_2O_2 production. Also, using the fluorometric method at pH 6.5, no H_2O_2 was observed when 5 or more Fe^{2+} ions were added to HoSF, indicating that the formation of H_2O_2 is not enhanced at the lower pH, where the rate of Fe^{2+} oxidation is significantly decreased.

H_2O_2 Production under Nonsaturating O_2 Conditions. Because the results in Figure 1 were achieved in vigorously stirred reaction vials with saturating air, such conditions may have minimized H_2O_2 production in favor of reaction 2. To test this possibility, the reaction of Fe^{2+} with HoSF was conducted under two other sets of conditions in which (1) O_2 was in moderate excess (~4 O_2/Fe^{2+}) but not continually saturating and (2) O_2 reacted with stoichiometric (2 Fe^{2+}/O_2) or with excess Fe^{2+} (O_2 was limiting). Figure 2 summarizes the results of these reactions and their associated control reactions, all conducted at pH 7.5 and measured by the fluorometric method that gives maximum sensitivity for H_2O_2 detection. The results in Figure 2 correspond to a 10 min reaction interval at an Fe^{2+}/HoSF ratio of 10.0 and are consistent with the results in Figure 1 obtained under identical conditions with saturating air. Figure 2 shows that with nonsaturating O_2 the reaction of 10.0 Fe^{2+} with HoSF to form a small core does not produce H_2O_2 (lane 3). However, when a standard addition of H_2O_2 to a concentration of ~12 μM was made, the corresponding amount of H_2O_2 was readily detected (lane 6).

Simultaneous Assessment of O_2, H_2O_2, and Fe^{2+} Using DPP. By measurement of the amount of O_2 initially present in a Mops-buffered solution containing HoSF, and then addition of Fe^{2+} until all O_2 was consumed, there was no increase in current at −1095 mV, indicating that H_2O_2 was not formed during the reaction. When standard H_2O_2 was added, an increased current flow was observed, proportional to the amount of H_2O_2 added, establishing that if H_2O_2 had initially formed it would have been detected.

Simultaneous measurements of the O_2 concentration gave an Fe^{2+}/O_2 stoichiometry of ~3.6, suggesting that ~90% of the O_2 was reduced to H_2O during the iron deposition reaction. This value is approximate (4.0 is expected; see reaction 2) because during the 10 min Fe^{2+} oxidation interval, the turbulence caused by the movement of the electrode (drop dislodgment by the "drop knocker") caused a small loss of dissolved O_2. The absence of H_2O_2 formation is consistent with the O_2 being reduced to H_2O and not to H_2O_2 during HoSF-catalyzed Fe^{2+} oxidation.

Microcoulometry. Microcoulometry at −560 mV is a sensitive method (0.1 μM detection limit) for measuring the total number of reducing equivalents present in an anaerobic reaction mixture. Oxidation of Fe^{2+} by O_2, according to

Table 1: Microcoulometric Reduction of HoSF Containing Iron Atoms Deposited under Various Conditions at pH 7.5

reconstituted holo HoSF[a]	e/HoSF (measured)[b]	e/Fe predicted[c] from reaction 1	e/Fe (measured)
excess O_2 (11 Fe^{3+})	10.8 ± 0.6[d]	2.0	0.98 ± 0.05
excess O_2 (27 Fe^{3+})	27.3 ± 1.0[d]	2.0	1.01 ± 0.06
4.0 Fe^{2+}/O_2 (11 Fe^{3+})	9.2 ± 0.5	2.0	0.84 ± 0.05
2.0 Fe^{2+}/O_2 (11 Fe^{3+})	9.6 ± 0.5	2.0	0.87 ± 0.05
2.0 Fe^{2+}/O_2 (150 Fe^{3+})	148 ± 6	2.0	0.97 ± 0.04

[a] In the first two samples, 11.0 and 27.0 Fe^{2+} were oxidized in the presence of HoSF under air-saturation conditions. For the next two samples, 11.0 Fe^{2+} were oxidized under a moderate excess of O_2 (4.0 Fe^{2+}/O_2) and stoichiometric O_2 (2.0 Fe^{2+}/O_2). The last sample had 150 Fe^{2+} oxidized at an Fe^{2+}/O_2 ratio of 2.0. [b] The total number of electrons accepted by HoSF at pH 8.0 during microcoulometric reduction at −560 mV vs NHE. For each sample, six to eight separate measurements were taken and averaged. The error limits are given as the standard deviation. [c] The expected reduction stoichiometry if Fe^{2+} is oxidized by O_2 according to reaction 1, and both Fe^{3+} and H_2O_2 are reduced. [d] The apo HoSF used for sample preparation can be reduced by 5.3 ± 0.2 e/HoSF as determined by microcoulometry prior to iron deposition by O_2 oxidation. These centers remain oxidized in excess O_2, and a correction of 5.3 e/HoSF was subtracted from the measured e/HoSF values.

reaction 1, should produce 0.5 H_2O_2 as a byproduct for each Fe^{3+} deposited within HoSF. Reduction of this anaerobic solution should completely reduce both Fe^{3+} and H_2O_2 with a total reduction stoichiometry of 2 electron equivalents per Fe^{3+} according to reaction 1. Table 1 contains the results from microcoulometric reduction of HoSF samples prepared by oxidizing Fe^{2+} with O_2 under conditions of excess O_2, moderate levels of excess O_2 (∼4.0 Fe^{2+}/O_2), and limiting O_2 (2.0 Fe^{2+}/O_2) at Fe^{3+}/HoSF ratios of 11.0, 27.0, and 150. For HoSF prepared by oxidation of 11.0 Fe^{2+} by excess O_2, 16.1 electrons were required for complete reduction, indicating that 1.4 electrons were added per Fe^{3+}. However, when corrected for 5.3 redox centers initially present and readily oxidized by excess air in the apo HoSF (*17*, *18*), a value of 0.98 e/Fe^{3+} is obtained. For HoSF prepared with moderate or limiting O_2, 9.0−10.0 electrons are added, corresponding to a value of 0.8−0.9 e/Fe^{3+}. Values of <1.0 suggest that the Fe^{2+} may have reduced the oxidized protein centers initially present and that the low level of O_2 present was not capable of reoxidizing them. This seems likely because in all experiments, the addition of bipyridine showed that <10% of the added iron produced $[Fe(bipy)_3]^{2+}$, indicating that >90% of the Fe^{2+} was oxidized. Identical reactions were conducted at pH 6.5, but only reduction equivalent to the amount of Fe^{3+} present was observed. Addition of catalase did not change the extent of reduction, indicating that no additional oxidant (O_2) was produced by catalase, suggesting the absence of H_2O_2. Independent measurements demonstrated that added H_2O_2 was readily reduced under the microcoulometric conditions that were used. These microcoulometric measurements show that no additional oxidant was present beyond the Fe^{3+} formed in the HoSF core and rule out the production of H_2O_2 during the deposition of Fe^{3+}. The results are consistent with reaction 2 but not with reaction 1.

Sequential Addition of Fe^{2+}. Previous results (*10*, *14*) suggested that H_2O_2 is formed at the ferroxidase site in the H subunit and that the μ-dioxodiiron species formed during H_2O_2 formation cleared from the site within about 10 min (*14*). If this is the case, H_2O_2 should form and accumulate with each cycle of oxidation of Fe^{2+} by O_2. We conducted experiments to test this possibility by measuring the amount of H_2O_2 formed after each of 10 sequential additions of Fe^{2+} that should produce 60 μM H_2O_2 with each addition according to reaction 1. The results of these experiments showed that H_2O_2 does not accumulate as predicted and in fact is not formed at any point during sequential Fe^{2+} oxidation.

Catalase Activity of Apo and Holo HoSF. The possibility was examined that H_2O_2 may actually form as shown in reaction 1 but then rapidly decomposes into H_2O and O_2 by catalase activity inherent to apo or holo HoSF containing a small Fe^{3+} core. Using DPP and microcoulometry, we measured the stability of 28 μM H_2O_2 in the presence of 5 μM apo HoSF and holo HoSF containing 10 Fe^{3+} ions and found that less than 40% of the added H_2O_2 decomposed over a >60 min time interval. This weak catalase activity displayed for both apo and holo HoSF was not rapid enough to decompose enough H_2O_2 to explain the lack of H_2O_2 formation in the experiments reported here.

Iron Deposition Reactions with H_2O_2 as an Oxidant. The reaction of 10, 50, and 100 Fe^{2+} with HoSF under anaerobic conditions was conducted using H_2O_2 as an oxidant to determine if H_2O_2 is a facile kinetic oxidant for HoSF-catalyzed iron deposition. An identical set of control reactions was conducted except HoSF was absent. For reactions both in the presence and in the absence of HoSF, rapid oxidation of Fe^{2+} to Fe^{3+} occurs, but $Fe(OH)_3$ precipitated in the control reaction within ∼1.0 min which, when centrifuged, left a clear supernatant solution containing less than 5% of the original iron. In contrast, Fe^{2+} oxidation by H_2O_2 in the presence of HoSF formed no $Fe(OH)_3$ precipitate but produced a clear solution of holo HoSF containing >90% of the added iron. These results show that H_2O_2 rapidly oxidizes Fe^{2+} with subsequent deposition of $Fe(OH)_3$ within the HoSF core, and this result suggests that if H_2O_2 is formed during iron deposition, it would undergo rapid reduction by Fe^{2+} to form H_2O and not accumulate in solution. Such a series of reactions would produce a reaction stoichiometry consistent with reaction 2.

It should be noted that for oxidation of 100 Fe^{2+} by H_2O_2, HoSF remained stable and homogeneous for 3−4 h without any noticeable formation of $Fe(OH)_3$ or evidence of further reaction. However, after this time period slight turbidity began to develop, and after >10 h, a gelatinous precipitate containing most of the initially added iron and HoSF formed. For the oxidation of 50 Fe^{2+}, about 20% of the protein precipitated after 10 h, but for the addition of 10 Fe^{2+}, no detectable precipitation was observed. These results suggest that H_2O_2 is capable of rapidly oxidizing Fe^{2+} and depositing it within HoSF, but at high levels of iron deposition (requiring high levels of H_2O_2), damage occurs to the protein by this oxidant. This behavior was not observed in a control reaction for the deposition of >500 Fe^{2+} with O_2 as an oxidant, suggesting further that free H_2O_2 is not formed in measurable quantities during the iron deposition and O_2 reduction reactions.

DISCUSSION

The iron deposition reaction in HoSF is a complex process consisting of several conceptually distinguishable steps such

Table 2: Calculated $\Delta G'$ and E' Values at 298 K for Reactions 1−3 at Selected pH Values[a]

	pH 6.5		pH 7.0		pH 7.5		pH 8.0	
reaction	$\Delta G'$ (kJ/mol of O_2)	E' (V)	$\Delta G'$ (kJ/mol of O_2)	E' (V)	$\Delta G'$ (kJ/mol of O_2)	E' (V)	$\Delta G'$ (kJ/mol of O_2)	E' (V)
1 ($n = 2$[b])	−76.4	0.396	−87.8	0.455	−99.3	0.515	−110.7	0.574
2 ($n = 4$)	−354.8	0.919	−377.6	0.978	−400.4	1.037	−423.2	1.096
3 ($n = 2$)	−278.4	1.442	−289.8	1.502	−301.1	1.560	−312.5	1.619

[a] The values are calculated from standard reduction potentials and apply to the indicated pH values. A strong pH dependence of 120 mV/pH unit is calculated for reactions 1−3 that favors Fe^{2+} oxidation with increasing pH. The standard state for solid $Fe(OH)_3$ for reactions 1−3 and that contained within the HoSF core were assigned an activity of 1.0. The $Fe(OH)_3$ contained within the HoSF core is likely stabilized by the protein environment relative to solid $Fe(OH)_3$ outside of the HoSF core. This effect would enhance development of $Fe(OH)_3$ within the core and make the $\Delta G'$ and E' values more favorable than those indicated above. [b] The n value in the Nernst equation indicates the number of electrons transferred in the reaction.

as the binding of Fe^{2+} to the protein, oxidation to Fe^{3+}, migration of Fe^{3+} to the ferritin interior, and hydrolysis of Fe^{3+} to form the ferrihydrite mineral core. Considerable effort has gone into elucidating the details of iron deposition through study of these individual reactions (*1*, *2*, *5*, *10*, *14*, *19*, *20*). An overview has emerged proposing that iron deposition is a biphasic process consisting of two mechanistically distinct reactions with the distinguishing O_2 reduction stoichiometries (*10*, *14*) described by reactions 1 and 2.

At low levels of iron loading, Fe^{2+} oxidation is proposed (*10*, *14*) to occur by reaction 1 at the ferroxidase centers contained within the H subunit of HoSF. For this reaction, stoichiometric measurements reported that 2 Fe^{2+} are oxidized per O_2, with H_2O_2 as a predicted product. Besides these detailed stoichiometric and kinetic results, spectroscopic studies described the formation of a short-lived diferric peroxo intermediate that rapidly decayed to free H_2O_2 (*21*−*23*). Thus, the long-held view that H_2O_2 is a product of O_2 reduction during ferritin function has some supportive experimental evidence in the form of this peroxo intermediate. However, with the exception of the characterized peroxo intermediate, and its proposed subsequent decomposition into H_2O_2 (not observed in this study), no direct assessment of H_2O_2 has actually been reported.

The second iron oxidation process proposes that 4 Fe^{2+} are oxidized by O_2 on the mineral core surface (*7*, *10*, *14*) with formation of H_2O as the product of O_2 reduction. This view also has a long history, as early kinetic studies of the iron deposition reactions were interpreted as a mineral surface catalytic process (*24*). Consistent with this view is a recent study (*25*) that shows that the surface of the mineral core has novel redox reactivity, especially with phosphate present. Thus, both mechanistically distinct reactions comprising the Fe^{2+} oxidation reactions catalyzed by HoSF seem to have supporting experimental evidence.

The study presented here was initiated to confirm the presence of H_2O_2 and gain mechanistic information about the proposed ferroxidase and mineral surface reactivity pathways described by reactions 1 and 2. However, each of the independent methods that was used did not detect H_2O_2 as a product at Fe^{2+}/HoSF ratios as low as 5.0 or at short reaction times of ∼10 s. Amounts of H_2O_2 only comparable to those in control reaction mixtures lacking H_2O_2 were observed. Therefore, we conclude that H_2O_2 is not a product of the iron deposition reaction as predicted by equation 1. Microcoulometric results support this conclusion and indicate that reduction only equivalent to the Fe^{3+} present occurs (Table 1).

Table 2 and direct assessments using H_2O_2 as an oxidant show that reaction 3 is favorable and readily occurs, so H_2O_2 should be completely reduced to H_2O.

$$2Fe^{2+} + H_2O_2 + 4H_2O = 2Fe(OH)_3 + 4H^+ \qquad (3)$$

Consequently, H_2O_2 is not an expected product of the iron deposition reaction in HoSF using O_2 as an oxidant, a result experimentally confirmed in this study.

The absence of H_2O_2 formation stands in contrast to detailed studies predicting formation of stoichiometric amounts of H_2O_2 at low Fe loading values (*10*, *14*) according to reaction 1. H^+/Fe^{2+} values of 2.0 reported here confirm previous results (*14*) and are consistent with reaction 1, but this result is ambiguous because it is also consistent with reaction 2. From the input stoichiometry at low iron loading levels, H_2O_2 is predicted (*10*, *14*) to be the product of O_2 reduction, but from the output stoichiometry reported here, H_2O_2 is not detected.

These conflicting results indicate that the iron deposition reaction at low iron loading levels of ∼5−100 may be more complex than originally predicted, and we consider several possible explanations that might resolve these discrepancies and inconsistencies.

Methods Could Be Flawed. It is possible that the methods used to determine the input (2.0 Fe^{2+}/O_2) or output stoichiometry (no H_2O_2 formation) give incorrect results. An error in either set of measurements would resolve the disagreement, but this does not seem likely at the present time. The independent electrode oximetry and mass spectroscopic methods used in establishing the input Fe^{2+}/O_2 stoichiometry of 2.0 (*10*, *14*) are precise and well-established methods for O_2 assessment. Likewise, the three H_2O_2-specific and independent methods used here for H_2O_2 quantitation are very sensitive, and do not display interference reactions under the conditions that were used. All three methods show that H_2O_2 is not formed during the HoSF-catalyzed iron deposition reaction. The independent microcoulometric method also confirms the lack of H_2O_2 formation. If we accept the possibility that the methods used for defining the input and output stoichiometries for the iron deposition reaction are sound and accurately represent the reaction, then it is necessary to focus on the system itself for plausible explanations for the observed discrepancies. Since the system is composed of two distinct components (the protein component and the mineral core), we consider possible reactions involving each that might offer a plausible explanation that will reconcile previous results with those reported here.

H_2O_2 Is Formed Transiently. It is possible that H_2O_2 is initially produced but rapidly oxidizes the protein portion of HoSF. A precedent for HoSF protein oxidation has been reported (*17*) in which a protein redox center (containing tryptophan 93 in the H subunit) is reversibly oxidized. Three to six such centers are present in HoSF and could react with limited H_2O_2. Such a reaction would imply that H_2O_2 is initially produced but is not detected because it is immediately consumed by this secondary protein oxidation reaction and could explain an input stoichiometry consistent with reaction 1 but not produce free H_2O_2. However, there are only a small number of redox centers present in HoSF (3.0−6.0), and if this reaction occurs, only a small amount of H_2O_2 (1.5−3.0 H_2O_2/HoSF) would be consumed by this process. For oxidation of 8−20 Fe^{2+}/HoSF, 4−10 H_2O_2 should form, an amount larger than the capacity of the protein-bound redox centers. This amount of Fe^{2+} oxidation should produce H_2O_2 in excess of the capacity of these centers and produce measurable H_2O_2, but none is observed.

The possibility that H_2O_2 is initially formed but decomposes by the inherent catalase activity of HoSF itself or its mineral core was shown not to be a likely explanation because H_2O_2 is quite stable in the presence of each, decomposing only ∼40% in >1 h. If some other process decomposes H_2O_2, it must do so within 10 s of formation as we were unable to detect any H_2O_2 formation after this time interval.

H_2O_2 Could Remain Bound. Another possible explanation is that H_2O_2 or its stoichiometric equivalent forms a stable intermediate and remains bound to or is occluded by the developing mineral core. Such a species would not release free H_2O_2 into solution and would go undetected by methods 1 and 3 used to directly measure the amount of H_2O_2, but would still require an Fe^{2+}/O_2 ratio of 2.0 for its formation. However, assessment of H_2O_2 by method 2 requires addition of HoSF to 1.0 M HCl for development of I_3^- by H_2O_2 oxidation of I^-. These conditions favor HoSF dissociation into its subunits and dissolution of the FeOOH mineral core, providing conditions for decomposition of simple peroxo intermediates and releasing H_2O_2. Figure 1 shows no H_2O_2 formation by method 2, suggesting that a simple H_2O_2 intermediate is not likely present. Microcoulometry also excludes the presence of a stable *redox-active*, peroxo intermediate; a redox inactive species would not be detected by this method, but such a species seems to be unlikely. The possibility that μ-dioxodiiron(IV) forms was also ruled out because such species are redox active and the microcoulometric results show e/Fe values of 1.0, not 2.0 or 4.0 as would be expected. Mössbauer spectra of HoSF containing small numbers of iron atoms (26−28) do not have the characteristic spectral parameters associated with Fe(IV). The presence of a peroxo-like intermediate present at significant concentrations during the iron deposition reaction is not consistent with the results reported here.

Experimental Conditions. The experiments reported here were conducted under nearly the same HoSF concentrations, buffer types and concentrations, and pH values and within the same temperature range as those experiments reporting Fe^{2+}/O_2 values of 2.0 (*10*, *14*). It does not seem reasonable that differences in experimental conditions offer an explanation for the discrepancies, and we are unable to account for the predicted formation of H_2O_2 and the absence of a measurable amount of H_2O_2 under the conditions used in our experiments.

The focus of this study was on assessment of H_2O_2 formed during the HoSF-catalyzed iron deposition reaction and not on the O_2 consumption stoichiometry. However, from two sets of experiments, we are able to suggest an answer to the important question of what the likely product of O_2 reduction is for the experiments reported here. Both the microcoulometry and DPP methods readily reduce O_2 and consequently are of value in determining its concentration in solution. Using the DPP method, an Fe^{2+}/O_2 value of ∼3.6 was observed, suggesting that O_2 is likely reduced to H_2O. The microcoulometric measurements support this conclusion. In addition, Table 2 and experiments using H_2O_2 as an oxidant to deposit iron in HoSF suggest that if H_2O_2 were formed, Fe^{2+} would reduce it to H_2O. The results reported here strongly suggest that our inability to assess H_2O_2 formation under the conditions we have examined is consistent with O_2 being reduced to H_2O as outlined by reaction 2.

REFERENCES

1. Proulx-Curry, P. M., and Chasteen, N. D. (1995) Molecular Aspects of Iron Uptake and Storage in Ferritin, *Coord. Chem. Rev. 144*, 347−368.
2. Ford, G. C., Harrison, P. M., Rice, D. W., Smith, J. M. A., Treffry, A., White, J. L., and Yariv, J. (1984) Ferritin Design and Formation of an Iron Storage Molecule, *Philos. Trans. R. Soc. London, Ser. B 304*, 551−566.
3. Harrison, P. M., and Arosio, P. (1996) The Ferritins: Molecular Properties, Iron Storage Function and Cellular Regulation, *Biochim. Biophys. Acta 1275*, 161−203.
4. Theil, E. C. (1987) Ferritin Structure Gene Regulation and Cellular Function in Animals Plants and Microorganisms, *Annu. Rev. Biochem. 56*, 289−316.
5. Crichton, R. R., and Charloteaux-Wauters, M. (1987) Iron Transport and Storage, *Eur. J. Biochem. 164*, 485−506.
6. Rice, D. W., Ford, G. C., White, J. L., Smith, J. L., Harrison, J. M. A., Urushizaki, P. M. I., Aisen, P., and Listowsky, I. (1983) Recent advances in the three-dimensional structure of ferritin, *Struct. Funct. Iron Storage Transp. Proteins, Proc. Int. Conf., 6th*, 11−16.
7. Macara, I. G., Hoy, T. G., and Harrison, P. M. (1972) The Formation of Ferritin from Apo Ferritin Kinetics and Mechanism of Iron Uptake, *Biochem. J. 126*, 151−162.
8. Lawson, D. M., Treffry, A., Artymiuk, A. P. J., Harrison, P. M., Yewdall, P. M. S. J., Luzzago, A., Cesareni, G., Levi, S., and Arosio, P. (1989) Identification of the Ferroxidase Center in Ferritin, *FEBS Lett. 254*, 207−210.
9. Hempstead, P. D., Hudson, A. J., Artymiuk, P. J., Andrews, S. C., Banfield, M. J., Guest, J. R., and Harrison, P. M. (1994) Direct observation of the iron binding sites in a ferritin, *FEBS Lett. 350*, 258−262.
10. Xu, B., and Chasteen, N. D. (1991) Iron Oxidation Chemistry in Ferritin. Increasing Fe/O_2 Stoichiometry during Core Formation, *J. Biol. Chem. 266*, 19965−19970.
11. Sun, S., Arosio, P., Levi, S., and Chasteen, N. D. (1993) Ferroxidase Kinetics of Human Liver Apoferritin Recombinant H-chain Apoferritin and Site-Directed Mutants, *Biochemistry 32*, 9362−9369.
12. Sun, S., and Chasteen, N. D. (1994) Rapid kinetics of the EPR-active species formed during initial iron uptake in horse spleen apoferritin, *Biochemistry 33*, 15095−15102.
13. Sun, S., and Chasteen, N. D. (1992) Ferroxidase Kinetics of Horse Spleen Apoferritin, *J. Biol. Chem. 267*, 25160−25166.
14. Yang, X., Chen-Barrett, Y., Arosio, P., and Chasteen, N. D. (1998) Reaction Paths of Iron Oxidation and Hydrolysis in Horse Spleen and Recombinant Human Ferritins, *Biochemistry 37*, 9743−9750.

15. Waldo, G. S., Ling, J., Sanders-Loehr, J., and Theil, E. C. (1993) Formation of an Iron-III Tyrosinate Complex During Biomineralization of H-Subunit Ferritin, *Science 259*, 796−798.
16. Zhou, M., Diwu, Z., Panchuk-Voloshina, N., and Haugland, R. P. (1997) A Stable Nonfluorescent Derivative of Resorufin for the Fluorometric Determination of Trace Hydrogen Peroxide: Applications in Detecting the Activity of Phagocyte NADPH Oxidase and Other Oxidases, *Anal. Biochem. 253*, 162−168.
17. Watt, G. D., and Frankel, R. B. (1991) Redox Capacity of Apo Mammalian Ferritin, in *Iron Biominerals*, pp 307−313, Plenum Press, New York.
18. Watt, R. K., Frankel, R. B., and Watt, G. D. (1992) Redox Reactions of Apo Mammalian Ferritin, *Biochemistry 31*, 9673−9679.
19. Harrison, P. M., Hempstead, P. C., Artymiuk, P. J., and Andrews, S. C. (1998) Structure−Function Relationships in the Ferritins, *Met. Ions Biol. Syst. 35*, 435−478.
20. Theil, E. C., and Aisen, P. (1987) The Storage and Transport of Iron in Animal Cells, in *Iron Transport in Microbes, Plants and Animals* (Winkelmann, G., Van Der Helm, D., and Neilands, J. B., Eds.) p 533, VCH Publishers, New York.
21. Moenne-Loccoz, P., Krebs, C., Herlihy, K., Edmondson, D. E., Theil, E. C., Huynh, B. H., and Loehr, T. M. (1999) The Ferroxidase Reaction of Ferritin Reveals a Diferric μ-1,2 Bridging Peroxide Intermediate in Common with Other O_2-Activating Non-Heme Diiron Proteins, *Biochemistry 38*, 5290−5295.
22. Pereira, A., Small, W., Krebs, C., Tavares, P., Edmondson, D., Theil, E., and Huynh, B. (1998) Direct spectroscopic and kinetic evidence for the involvement of a peroxodiferric intermediate during the ferroxidase reaction in fast ferritin mineralization, *Biochemistry 37*, 9871−9876.
23. Hwang, J., Krebs, C., Huynh, B. H., Edmondson, D. E., Theil, E. C., and Penner-hahn, J. E. (2000) A short Fe−Fe distance in Peroxodiferric Ferritin: Control of Fe Substrate Versus Cofactor Decay? *Science 287*, 122−125.
24. Treffry, A., and Harrison, P. M. (1979) The Binding of Iron-(III) By Ferritin, *Biochem. J. 181*, 709−716.
25. Johnson, J. L., Cannon, M., Watt, R. K., Frankel, R. B., and Watt, G. D. (1999) Forming the Phosphate Layer in Reconstituted Horse Spleen Ferritin and the Role of Phosphate in Promoting Core Surface Redox Reactions, *Biochemistry 38*, 6706−6713.
26. Bauminger, E. R., Harrison, P. M., Hechel, D., Nowik, I., and Treffry, A. (1994) How does the ferritin core form? *Hyperfine Interact. 91*, 835−839.
27. Bauminger, E. R., Harrison, P. M., Hechel, D., Nowik, I., and Treffry, A. (1991) Mössbauer Spectroscopic Investigation of Structure−Function Relations in Ferritins, *Biochim. Biophys. Acta 1118*, 48−58.
28. Bauminger, E. R., Harrison, P. M., Hechel, D., Hodson, N. W., Nowik, I., Treffry, A., and Yewdall, S. J. (1993) Iron(II) oxidation and early intermediates of iron-core formation in recombinant human H-chain ferritin, *Biochem. J. 296*, 709−719.

BI001981V